Virology 412 (2011) 91–100

Contents lists available at ScienceDirect

Virology

journal homepage: www.elsevier.com/locate/yviro

Neonatal rhesus monkey is a potential animal model for studying pathogenesis of EV71 infection

Longding Liu [a,1], Hongling Zhao [a,1], Ying Zhang [a], Jingjing Wang [a], Yanchun Che [a], Chenghong Dong [a], Xuemei Zhang [a], Ruixiong Na [a], Haijing Shi [a], Li Jiang [a], Lichun Wang [a], Zhongping Xie [a], Pingfang Cui [a], Xiangling Xiong [b], Yun Liao [a], Shudong Zhao [a], Jiahong Gao [a], Donghong Tang [a], Qihan Li [a,*]

[a] Institute of Medical Biology, Chinese Academy of Medicine Science, Kunming 650118, PR China
[b] Kunming Medical University, Kunming 650032, PR China

ARTICLE INFO

Article history:
Received 26 October 2010
Returned to author for revision
30 November 2010
Accepted 30 December 2010
Available online 22 January 2011

Keywords:
Enterovirus 71 (EV71)
Hand–foot–mouth disease (HFMD)
Neonatal rhesus monkey
Animal model
Pathogenesis

ABSTRACT

Data from limited autopsies of human patients demonstrate that pathological changes in EV71-infected fatal cases are principally characterized by clear inflammatory lesions in different parts of the CNS; nearly identical changes were found in murine, cynomolgus and rhesus monkey studies which provide evidence of using animal models to investigate the mechanisms of EV71 pathogenesis. Our work uses neonatal rhesus monkeys to investigate a possible model of EV71 pathogenesis and concludes that this model could be applied to provide objective indicators which include clinical manifestations, virus dynamic distribution and pathological changes for observation and evaluation in interpreting the complete process of EV71 infection. This induced systemic infection and other collected indicators in neonatal monkeys could be repeated; the transmission appears to involve infecting new monkeys by contact with feces of infected animals. All data presented suggest that the neonatal rhesus monkey model could shed light on EV71 infection process and pathogenesis.

Introduction

Enterovirus 71 (EV71) is commonly recognized as the main human pathogen of hand–foot–mouth disease (HFMD), occasionally causing severe fatality (Ooi et al., 2007). Several severe epidemic outbreaks involving large groups within populations have occurred globally, specifically in Asia-Pacific regions, since the 1990s (CDC, 1998; Chan et al., 2000; Shimizu et al., 1999). Notably, though mild clinical manifestations of HFMD are characterized as papules, vesicles or petechiae of hand, foot and mouth in millions of patients (Ho et al., 1999; Liu et al., 2000); a considerable number of people, specifically infants and young children, infected by EV71 develop severe disease (Ho et al., 1999; McMinn, 2002). In the outbreaks of HFMD involving hundreds of thousands of cases in Taiwan from 1999 to 2001, several hundreds of fatal cases with high mortality in young children were reported (Ho et al., 1999; Lin et al., 2003b). From 2008 to 2010, an average of several hundreds of deaths caused by EV71 infection in young children are reported each year in the Chinese Mainland (Ding et al., 2009; Xu et al., 2010; Yang et al., 2009). Most of the fatal cases caused by EV71 infection are typically associated with neural diseases and complications of the central nervous system (CNS) and subsequently lead to pulmonary edema and function collapse due to rapid development and progress of disease (Lin et al., 2006), which makes clinical treatment of such acute viral-induced diseases challenging (Lin et al., 2006). Though mechanisms of neuropathogenesis in enteroviral infections, poliovirus infection for example, have been extensively described in many studies (Couderc et al., 1989; Whitton et al., 2005), the potential pathogenesis of EV71 infection remains unknown. Results from limited autopsies demonstrate that pathological changes in EV71-infected fatal cases are principally characterized by clear inflammatory lesions in the oblongata, hypothalamus, spinal cord and other parts of the CNS in a pattern of neural cell necrosis, degeneration, local inflammatory cell infiltration, perivascular cuffing formation and so on (Wong et al., 2008). In contrast, the typical clinical symptoms in non-neural organs exhibit the development of pulmonary edema (Hsueh et al., 2000), which can frequently lead to deaths in young children. It is generally believed that the study of the pathogenesis of EV71 infection in clinical patients could be extremely difficult compared to studies in different animal models that have already documented significant advances in further characterizing the pathogenesis of EV71 infection (Nagata et al., 2002; Ong et al., 2008). A study in a murine model indicates that the challenge of adapted mutants such as the MAVS strain (Wang et al., 2004) can lead directly to flaccid paralysis or death of mice and

* Corresponding author. Institute of Medical Biology, Chinese Academy of Medicine Science and Peking Union Medical College, 379 Jiaoling Road, Kunming, Yunnan, PR China, 650118. Fax: +86 871 8334483.
E-mail address: imbcams.lq@gmail.com (Q. Li).
[1] Longding Liu and Hongling Zhao contributed equally to this work.

0042-6822/$ – see front matter © 2011 Elsevier Inc. All rights reserved.
doi:10.1016/j.virol.2010.12.058

corresponding pathological changes in CNS (Ong et al., 2008; Wang et al., 2004). Likewise, challenge with a temperature resistant mutant (tr strain) in cynomolgus monkeys can induce symptoms of neurological disorders, such as flaccid paralysis and ataxia, as well as corresponding pathological changes in CNS (Hashimoto and Hagiwara, 1983). These data provide evidence that using animal models in the study of the development of EV71 vaccines and anti-viral drugs could be fruitful. However, as a result of the limits of the modified viral strains, when compared to natural human viral infection, the potential pathogenesis process of EV71 infection in its natural host cannot be sufficiently defined by current data.

We have previously studied the possibility of using rhesus monkeys as an animal model for EV71 infection by an EV71 strain isolated from a patient with HFMD through different EV71-infected routes of the intracerebral, intravenous, respiratory and intestinal systems. As shown in the dynamic and comprehensive pathogenic analysis and histopathological examination on adult rhesus monkeys, the basic pathogenesis process of EV71 infection includes exhibition of regular viremia, specific virus dynamic profile and subsequent major neuropathological changes in the CNS (Zhang et al., Submission); the preference of EV71 to respiratory infection has been sufficiently demonstrated, despite a lack of typical clinical manifestations of HFMD like papules, vesicles or petechiae and even flaccid paralysis in the severe cases. On the basis of these data and investigations of EV71-infected humans, it is generally believed that animals, particularly non-human primates, could be useful in mimicking the EV71 infectious process. Studying EV71 infection in these animal models would provide more data about the pathogenesis of EV71 infection in humans. In the light of this, our work is further focused on the study of the EV71 infectious process in neonatal rhesus monkeys; we analyzed the virus dynamic profile, corresponding pathological changes in some organs and the resulting clinical manifestations. Additionally, we succeeded in replicating the infectious process in new rhesus monkeys using feces of EV71-infected neonatal monkeys. These findings appear to suggest that neonatal rhesus monkeys could potentially be used as an effective animal model for EV71 infection in the development of new drugs and vaccines, which might provide new insights into understanding EV71 infection and its associated pathogenesis.

Results

Clinical manifestations in EV71-infected neonatal rhesus monkeys

In our previous studies of EV71-infected adult monkeys, neither typical neurological symptoms in EV71-infected animals nor the papules or vesicles on limbs and mouths found in EV71-infected humans were observed. The only clinical sign was of body temperature elevation (Supplemental Table 1) (Zhang et al., Submission). In the current study, the typical flaccid paralysis was not noticed in infected neonates, but slight muscle tension decreased from days 7

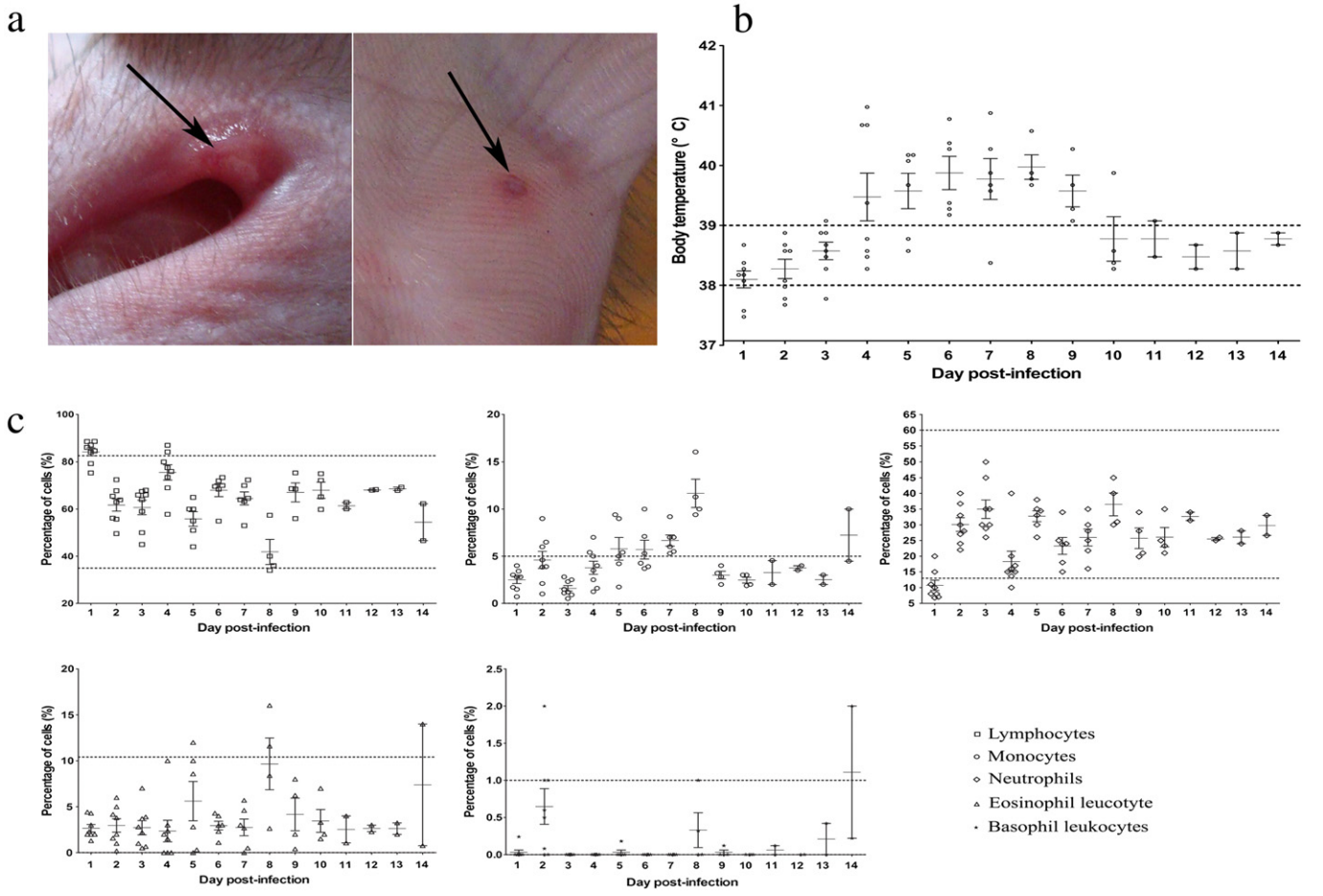

Fig. 1. Clinical manifestations of neonatal rhesus monkey infected by EV71 via respiratory route. 8 monkeys were challenged with EV71 ($10^{4.5}$ $CCID_{50}$/monkey) and 2 monkeys were used as uninfected negative controls. (a) Vesicular lesions in the mouth and foot of newborn rhesus monkey. (b) Monitoring on body temperatures of rhesus monkeys infected by EV71. Body temperatures of infected monkeys were measured by anus rout twice each day post-infection. The normal body temperatures (data collected from two negative monkeys and referring Li, 2005) ranging from 38 to 39 °C were showed as dot line. (c) The blood cell analysis using FCM and number statistic measure of rhesus monkeys infected by EV71, containing lymphocytes, monocytes, neutrophils, eosinophilic leucocytes and basophilic leukocytes. The percentages of normal cells ranging (data collected from two negative monkeys and referring Sibley, 1974) were showed as dot line. Blood samples were collected in whole course of EV71 infection (1–14 days post-infection) for detecting the presence of certain inflammatory markers.

to 10 p.i.; some papules, vesicles or petechiae manifested on limbs or mouths (Fig. 1a) from days 3 to 8 p.i.; body temperatures increased to some extent from days 4 to 8 p.i. (Fig. 1b) and blood cell examination revealed an increased number of mononuclear cells in some monkeys (Fig. 1c). These observations suggested that, when compared with usual clinical symptoms in infected adult monkeys (Supplemental Table 1), the papules or vesicles manifested on limbs and mouths in neonates might result from the difference in age at infection. Such clinical signs are not identified in animal models of cynomolgus monkeys (Nagata et al., 2004) but are quite similar to those in human infants and young children and are confirmed by histopathological examination and pathogenic analysis (see later description). Interestingly, and for unknown reasons, the typical neurological complications including flaccid paralysis were not observed. Although the ataxia, paralysis and other typical features have been reported by Nagata in cynomolgus monkeys (Nagata et al., 2004), there are only a few clinical reports of flaccid paralysis being a main characterization in human cases of HFMD in recent outbreaks (Kung et al., 2007) regardless of some paralysis cases found in previous epidemics induced by B or C1 genotype virus in Europe (Kapusinszky et al., 2010; Ortner et al., 2009). However, the clinical features displayed in neonatal monkeys, such as papules or vesicles, fever, and inflammatory responses indicated in blood cell analysis, as well as clinical manifestations in EV71-infected humans (Li et al., 2002) lead to the conclusion that there are significant similarities between clinical features manifesting in EV71-infected neonatal monkeys and humans.

Dynamic profile of virus in tissues of non-neural systems of EV71-infected neonatal monkeys

It has been previously documented that enteroviruses, in particular poliovirus, are present in organs of the lymphatic system of humans at early stages of infection (Ouzilou et al., 2002). Additionally, as revealed in studies of EV71 infection in murine and cynomolgus monkey animal models, virus has been frequently found in organs of many non-neural systems such as blood, heart, lung, spleen and muscles (Arita et al., 2007; Chen et al., 2004), which has been shown in our previous work performed on adult rhesus monkeys (Zhang et al., Submission). In this study of EV71 infection in neonatal rhesus monkeys, we analyzed viral load profiles of tissues and organs with potential involvement in an EV71 infection. The results indicated that viremia of neonatal monkeys developed during the period from day 5 to day 8 p.i. were detected by qRT-PCR detection (Fig. 2a) and were subsequently confirmed by virus titration in tissue culture (Supplemental Fig. 1a). The peak time point of this viremia occurred at the same for viral secretion in the pharynx of neonates (Fig. 2b and Supplemental Fig. 1b). Virus was detected in feces from viremia development until day 14 p.i., when monkeys were sacrificed (Fig. 2b and Supplemental Fig. 1b). This appears to imply that viral replication in corresponding tissues of monkeys is triggered at the time of viremia manifestation. As indicated in the analysis of EV71 infection in lymphatic system, viral loads reached the highest level (Fig. 2c) from days 4 to 7 p.i., particularly in some specific lymph nodes like the

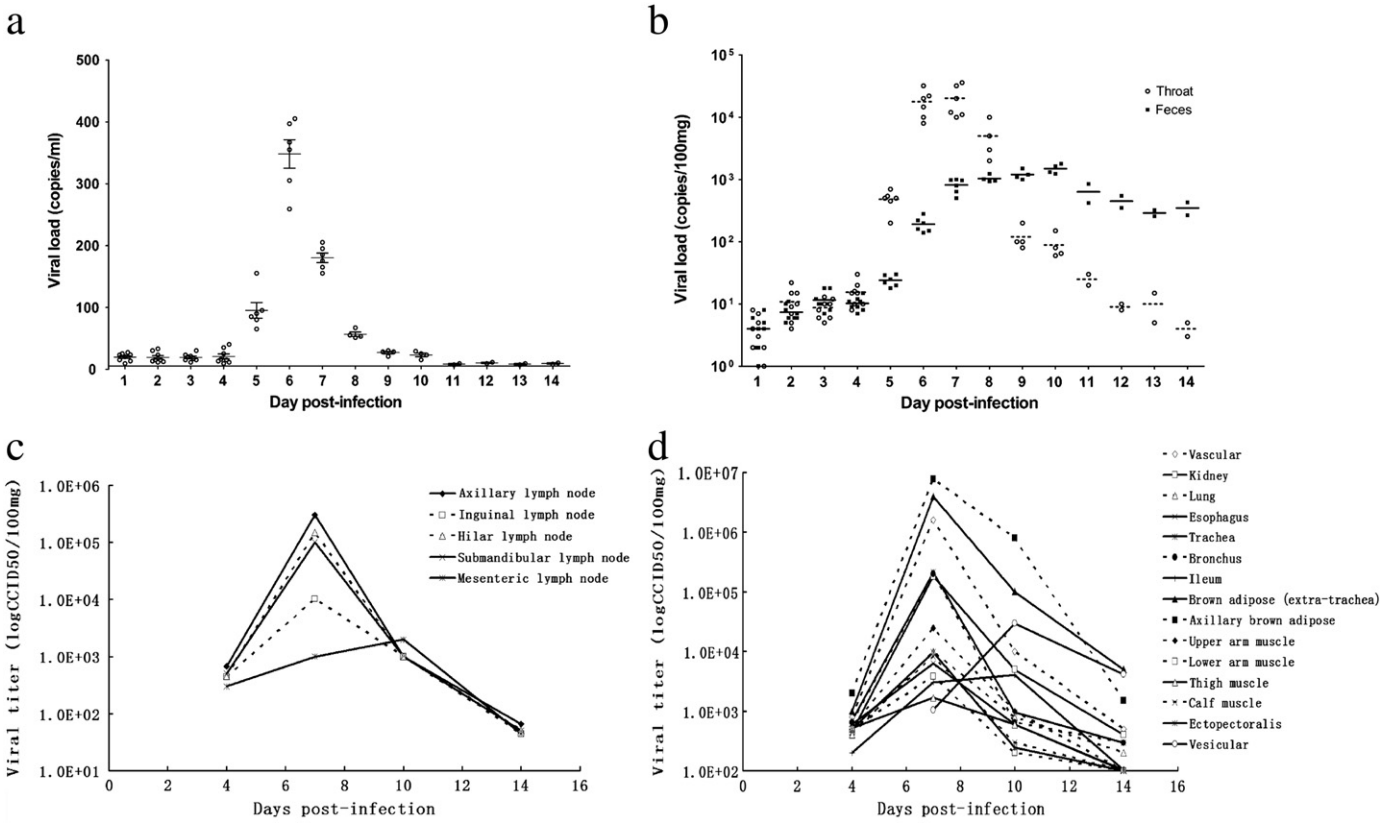

Fig. 2. Dynamic distribution of EV71 in infected neonatal rhesus monkey through respiratory route. 8 monkeys were challenged with EV71 ($10^{4.5}$ $CCID_{50}$/monkey) and 2 monkeys were used as uninfected negative controls. (a) Viral RNA was extracted from blood specimens and measured by Taqman based real-time qPCR assay, according to the procedure as described in manufacturer's protocol. Blood specimens were collected in whole course of EV71 infection (1–14 days post-infection). (b) Viral load in throat swabs and feces of infected rhesus monkeys. Throat swabs and stool specimens were collected in the whole course of EV71 infection (1–14 days post-infection). (c) Viral titration in lymphatic system of infected rhesus monkeys (axillary lymph node, mesenteric lymph node, inguinal lymph node, hilar lymph node and submandibular lymph node). (d) Viral titration in the major organs and tissues of infected rhesus monkeys (vascular, kidney, lung, esophagus, trachea, bronchus, ileum, brown adipose (beside trachea), axillary brown adipose, upper arm muscle, lower arm muscle, thigh muscle, calf muscle ectopectoralis and vesicular). Tissue specimens were collected from organs of these systems on days 4, 7, 10 and 14 post-infection. Viral copies were quantified according to vitro-synthesized RNA by spectrophotometry quantification, and the quantity was expressed as a relative copy number, determined by the equation [(μg of RNA/μl)/(molecular weight)] × Avogadro's number = viral copy number/μl. Viral titration was measured by a microtitration assay, according to the procedure as described in materials and methods. Values are the mean for 2 samples at each time point.

axillary lymph node, subsequently followed by gradual decline and load levels tended to be negative until day 14 p.i. (Fig. 2c). In addition to an increase in viral load levels in the lymph nodes, high viral load levels were detected in main organs, especially in some specific tissues of non-neural systems including: trachea, blood vessels, limb muscles, brown adipose and kidney (Fig. 2d). The highest viral-load level, 10^7 $CCID_{50}$/100 mg, was found in brown adipose tissue of axillary fossa and extra-trachea tissue. The electron microscopy analysis of brown adipose tissue showed an arrangement of viral particles in lines within the cells (Supplemental Fig. 2). A viral load level of 10^6 $CCID_{50}$/100 mg was found in the trachea and blood vessels, 10^3–10^4 $CCID_{50}$/100 mg in skeletal muscle, (Fig. 2d). As compared to previous results in adult monkeys (Supplemental Table 1) (Zhang et al., Submission), these findings suggest that peak viral load levels developed between days 4 and 7 p.i., in the organs and tissues which might eventually be the preferred target organs for infection, characterize EV71 infection in neonatal monkeys. Additionally, viral detection performed on papules or vesicles taken from mouths and limbs from days 5 to 8 p.i. further supported the growths' association with EV71 infection (Fig. 2d).

Viral distribution in the neural system of EV71-infected neonatal monkeys

The main target organs of EV71 infection in humans and other associated animal models has been identified to involve the central nervous system (CNS) (Lin et al., 2003a; Nagata et al., 2004; Ong et al., 2008; Wong et al., 2008) with infection characterized by clear neuropathological changes in a pattern of remarkable viral load distribution in the CNS (Ong et al., 2008; Wong et al., 2008). Several studies in murine models have suggested that EV71 is able to enter the CNS by transmission via peripheral nerves (PNS) using an active retrograde axonal transport route (Chen et al., 2007). In this work, general viral load distributions in the CNS and PNS were analyzed dynamically and some interesting findings were observed. The total distribution of viral loads tended to increase from day 7 p.i., peaked on day 10 p.i. followed by gradual decline (Fig. 3a), during which higher titers were distributed specifically in the medulla oblongata and thalamus. This distribution correlates with the observation of peak viral loads occurring in muscles, brown adipose and trachea organs on day 7 p.i. Additionally, as shown in viral load detection in trigeminal, brachial plexus, intercostal and sciatic nerves on 7 days p.i., peak viral loads were noticed in brachial plexus, intercostal nerves and followed by subsequent decline (Fig. 3b), which again correlates with brachial plexus and intercostal nerves that are directly linked to the PNS. This kind of potential time correlation is sufficient to support the hypothesis of EV71 transmission to CNS via peripheral nerves by using an active retrograde axonal transport route. Another marked finding is that EV71 was mainly detected in brachial plexus and in part within intercostal nerves in the PNS where higher viral loads were detected from days 4 to 7 p.i. Furthermore, these nerves are known to directly link to control body parts, including the neck, thorax and limbs, where tissues of axillary brown adipose and lymph nodes, upper arm muscle and pectoral muscle are found with the presence of high viral loads, which allows for an implication of correlated pathogenic process between viral infection routes and the infected CNS.

Features of pathological changes in EV71-infected neonatal monkeys

In our previous study of EV71 infection of adult rhesus monkeys, pathological changes were found in various organs of the animals, among which the most serious and severely infected ones were determined to be the wide range of CNS and respiratory system organs such as the trachea (Supplemental Table 1) (Zhang et al., Submission). This finding is consistent with other reports on neuropathological impairment of the CNS induced by EV71 infection in other animals (Arita et al., 2007; Chen et al., 2004; Ong et al., 2008). However, no pathological changes were documented in the respiratory systems of the animals. Whether the resistance of this tissue to change being caused by a failure in inoculation via respiratory route or other differences of biological properties of virus-adapted mutants remains unclear. In this study of EV71 infection in neonatal monkeys, pathological responses to EV71 infection were found in organs of the respiratory system such as the trachea and lungs, manifesting as epithelial cell damage and inflammatory cell infiltration (Fig. 4a); in contrast, pathological changes were not noticed in other main organs of the animals. Interestingly, marked inflammatory cell infiltration was noted in brown adipose and skeletal muscle tissue where viral load levels were very high (Fig. 4b). It is well known that brown adipose is far tissue specific to human infants and primate neonates and documented to be infected by poliovirus (Bodian, 1955;

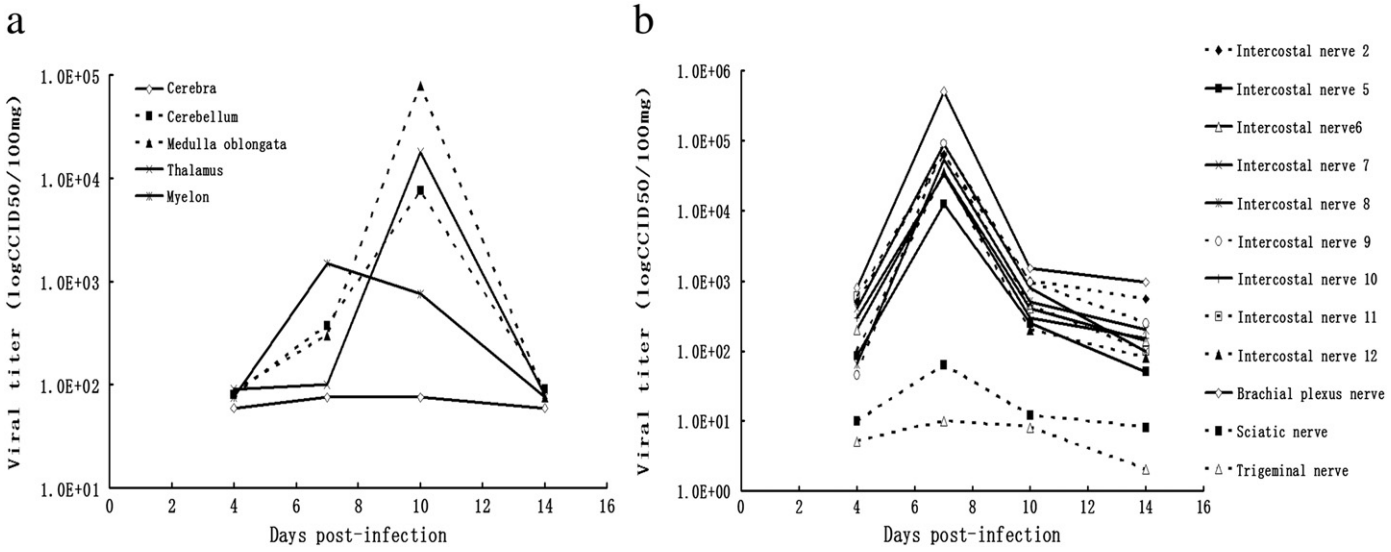

Fig. 3. Dynamic viral distribution in CNS and peripheral nerves of infected neonatal rhesus monkey through respiratory route. (a) Viral titration in CNS of infected rhesus monkeys (cerebra, cerebellum, medulla oblongata, pons and myelon). (b) Viral titration in peripheral nerves of infected rhesus monkeys (intercostals nerve 2, intercostals nerve 5–12, brachial plexus nerve, sciatic nerve and trigeminal nerve). Viral titration was measured by a microtitration assay, according to the procedure as described in Materials and methods. Tissue specimens were collected from organs of these systems on days 4, 7, 10 and 14 post-infection. Values are the mean for 2 samples at each time point.

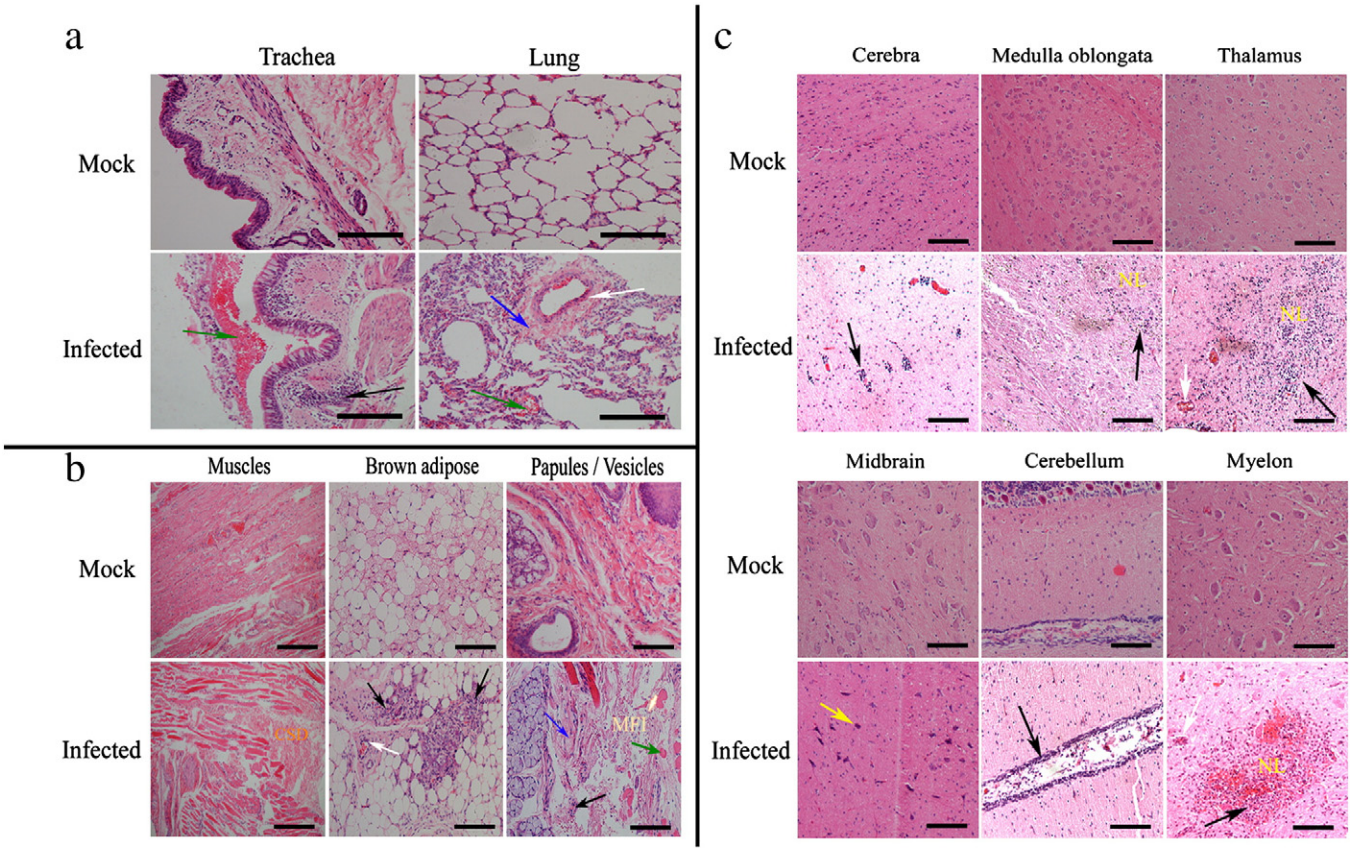

Fig. 4. Pathological changes in various tissues of neonatal rhesus monkey infected by EV71 via respiratory. (a) The typical features of pathological changes in respiratory apparatus (lung and trachea) of EV71 infected rhesus monkeys. Infiltration of inflammatory cells (black arrow), perivascular cuffing (white arrow), edema (blue arrow) and hemorrhage (green arrow). Images are shown at 200× magnification. Bar, 30 μm. (b) The typical features of pathological changes in muscles and brown adipose of EV71 infected rhesus monkeys. Infiltration of inflammatory cells (black arrow), perivascular cuffing (white arrow), edema (blue arrow), hemorrhage (green arrow), destruction of cell structure (yellow CSD) in muscles (100× magnification. Bar, 60 μm.), brown adipose tissues and vesicles (yellow MFI regions — "muscle fiber injury") (200× magnification. Bar, 30 μm.) were showed. (c) The typical features of pathological changes in CNS (cerebra, medulla oblongata, thalamus, midbrain, cerebellum and myelon) of EV71 infected rhesus monkeys. These images show infiltration of inflammatory cells (black arrow), perivascular cuffing (white arrow) and neuron retrogression (yellow arrow and NL regions — "neuronal lesions"). Images are shown at 200× magnification. Bar, 30 μm. Samples were collected on day 10 post-infection. The histopathological examinations were performed on 4-μm sections of paraffin-embedded tissue or organ stained with H&E according to the protocol.

Shwartzman et al., 1955). The high viral loads detected in brown adipose correlate with the presence of remarkable inflammatory changes (Fig. 2d). Additionally, as shown in histopathological examinations of papules or vesicles on mouths and limbs of EV71-infected monkeys (Fig. 4b), pathological changes associated with epithelial necrosis of subcutaneous small blood vessels and marked inflammatory cell infiltration in tissue structures were observed, implying that eruption of papules or vesicles in skin results from an inflammatory reaction of endothelial cells in subcutaneous small blood vessels in response to virus infection. However, the reason for their occurrence specifically on limbs requires further study. Again, the histopathological examination on the CNS revealed neuropathological lesions in the medulla oblongata, thalamus and gray matter of the spinal cord, which might contribute to degeneration of neural

Table 1
Neuropathological evaluation in CNS of newborn rhesus monkeys infected via respiratory route.

Infection rout	Dose	Monkey ID	Neuropathological symptoms[a] (days post infection)																									
			Brain														Spinal cord											
			Cerebra				Thalamus				Midbrain				Medulla oblongata				Cervical				Thorax				Lumbar			
			4	7	10	14	4	7	10	14	4	7	10	14	4	7	10	14	4	7	10	14	4	7	10	14	4	7	10	14
Respiratory	$10^{4.5}$	5410	1				2				1				2				1				1				1			
		5411		3				2				1				3				1				1				2		
		5412			3				4				2				4				2				1				0	
		5413				2				2				1				3				1				1				0
		5414	2				1				1				3				2				1				1			
		5415		2				1				3				2				2				2				1		
		5416			2				3				2				3				3				2				2	
		5417				2				1				1				1				1				0				1

[a] CNS lesions were scored according to the evaluation of extent of pathological change in CNS: 0, no lesion; 1, cellular infiltration; 2, cellular infiltration with minimal neural damage; 3, cellular infiltration with extensive neural damage; and 4, massive neural damage with or without cellular infiltration.

Table 2a
Clinical manifestations in EV71 respiratory infected new neonatal rhesus monkeys.

Pattern	Monkey ID	Clinical manifestations									
		Vesicular lesions[a]			Body temperature (°C) (days post infection)						
		Mouth	Hand	Foot	1	3	5	7	9	11	13
Infected new neonatal	5420	Y	Y	Y	38.5	38.1	39.2 ↑	39.8 ↑	40.5 ↑	39.3↑	38.7
	5421	Y	Y	N	37.7	38.2	39.5 ↑	40.3 ↑	39.9 ↑	39.0	38.9

↑: The temperature was upper than normal body temperatures ranging from 38 to 39 °C.
[a] Note: Y: yes or had; N: no or not had.

cells, perivascular infiltration and inflammatory cell aggregation etc. (Fig. 4c). All pathological examinations indicated that the most severe pathological changes were induced in a broad range of CNS tissues on day 10 p.i. (Table 1). Concomitantly, all pathological changes observed in all organs and tissues corresponded to viral antigen expression in associated tissues (Supplemental Fig. 3).

Infection of other individual neonates by feces of EV71-infected neonatal monkeys

Based on our previous studies in adult and neonatal rhesus monkeys (Supplemental Table 1), the respiratory tract is suggested as the potential main route for EV71 natural infection due to the high viremia in respiratory tissue during EV71 infection. Epidemiological studies in humans have further implicated the respiratory tract as a main route of EV71 transmission in human populations (Han et al., 2010). To determine the feasibility of using neonatal monkeys as an animal model for EV71 infection, 100 mg of feces taken from EV71-infected neonatal monkeys on day 10 p.i. were put in 5 ml PBS for sterilization and filtration. 500 μl of this solution was sprayed into the nasal passages of each of 4 neonates and the newly-infected monkeys were monitored for the aforementioned clinical signs and viral viremia development until day 14 p.i. when two of the monkeys were sacrificed for overall pathological and pathogenic examinations. The other two were reared for fecal examinations until day 30 p.i., during which time the associated neonates' breast-feeding female monkey were examined for viral loads in feces. Similar clinical manifestations, such as papules or vesicles and body temperature increasing, were exhibited (Table 2a), viremia developed between days 5 and 8 p.i. (Table 2b), and the virus was detected in the pharynx and feces (Table 2b). The pathological changes were observed in a wide range of CNS and respiratory tract tissues of neonates sacrificed on day 14 p.i. (Table 2c) with the same variety and severity as those characterized in the first group of neonates from the same time point. The biological events of infected neonatal monkeys, which are progress to development of complete pathological changes and advancement to infection of new individual neonate by fecal respiration, followed by induction of similar clinical manifestations in new individuals, are likely to support the significance of using neonatal rhesus monkeys as an animal model for EV71 infection.

Discussion

Many researchers have described in detail the pathogenesis of enteroviruses, particularly poliovirus, Coxsackie A and B and hepatitis A viruses in humans (Asher et al., 1995; Mena et al., 2000; Racaniello, 2006), the study of which will benefit greatly from the development of animal models in non-primates and mice for enterovirus infection (Chen et al., 2004). The precedent for animal models in studying enterovirus has been clearly demonstrated during the work on poliovirus and development of the polio vaccine (Dragunsky et al., 1996; Horie et al., 1994). With regard to the EV71 infectious disease and its unknown pathogenesis, development of animal models using primates with a close genetic relationship to humans will facilitate the study of EV71 pathogenesis. Our previous work has characterized the EV71 infectious process and its associated pathological changes in adult rhesus monkeys (Supplemental Table 1) (Zhang et al., Submission). The clinical manifestations, variety of viral load distributions and corresponding pathological features are discussed in the current study, further demonstrating the feasibility of using neonatal rhesus monkeys as an animal model for EV71 infection.

The clinical features in EV71-infected neonatal monkeys, in addition to general signs of fever, were pathological changes characterized by typical vesicles or papules on limbs and mouth (Fig. 1) and were confirmed to be similar to that in human patients with HFMD (Ho et al., 1999). Such changes are described for the first time in animal models for EV71 infection. The pathogenic analysis showed a viral load of over 10^3 $CCID_{50}$/100 mg in tissues of vesicles or papules (Fig. 2). The histopathological examination of these tissues clearly showed central pathological lesions in small blood vessel walls of subcutaneous tissues and tremendous inflammatory cell infiltration (Fig. 4b), linking EV71 infection to tissues of blood vessels (Fig. 2). On the contrary, there were no clear histopathological lesions in blood vessel endothelia of great blood vessels where high viral loads were detected (Fig. 2), which might be explained by difficulties in generating local inflammatory cell aggregation due to rapid blood flow in great vessels. In subcutaneous small blood vessels with a slow blood flow, virus might induce infection of endothelia upon attaching to blood vessel walls, and this perhaps leads to local inflammatory cell aggregation in response to various released inflammatory factors (Compton et al., 2003). Despite the advances presented, further work

Table 2b
Dynamic distribution of EV71 in infected new neonatal rhesus monkeys through respiratory route.

Pattern	Monkey ID	Dynamic distribution[a]	Days post infection													
			1	2	3	4	5	6	7	8	9	10	11	12	13	14
Infected new neonatal	5420	Viremia	−	−	−	+	++	+++	+++	+++	++	+	±	−	−	−
		Throat swab	−	−	−	+	++	+++	++++	++++	+++	+	−	−	−	−
		Feces	−	−	−	±	+	++	+++	++++	+++	+++	++	+++	++	+++
	5421	Viremia	−	−	−	±	+	+++	++++	++	++	−	−	−	−	−
		Throat swab	−	−	−	−	+	++	++++	+++	++	+	−	−	−	−
		Feces	−	−	−	−	+	++	++++	+++	+++	++	+++	++	++	++

−: copies ≤ 10^0; ±: copies ≤ 10^1; +: copies ≤ 10^2; ++: copies ≤ 10^3; +++: copies ≤ 10^4; ++++: copies ≥ 10^4.
[a] Note: Measured viruses load by Taqman based real-time qPCR assay, according to the procedure as described in manufacturer's protocol.

Table 2c
Pathological changes in CNS and respiratory tissues of new neonatal rhesus monkeys infected via respiratory route.

Pattern	Monkey ID	Pathological changes in different organs (days post infection)										
		CNS[a]								Respiratory tissues[b]		
		Cerebra	Thalamus	Midbrain	Medulla oblongata	Pons	Cervical	Thorax	Lumbar	Lung	Trachea	Bronchus
Infected new neonatal	5420	1	2	2	3	3	2	2	1	1	–	–
	5421	2	3	1	1	2	1	1	1	2E	1	1

Samples were collected on day 14 post-infected.
[a] CNS lesions were scored according to the evaluation of extent of pathological change in CNS: 0, no lesion; 1, cellular infiltration; 2, cellular infiltration with minimal neural damage; 3, cellular infiltration with extensive neural damage; and 4, massive neural damage with or without cellular infiltration.
[b] Note: E: edema and/or hemorrhage. 1: cellular infiltration; 2: cellular infiltration and damage of tissue; 3: massive cellular infiltration and severe damage of tissue; –: no obvious pathological change.

is required to elucidate the details of the pathological and physiological mechanisms of these lesions in skin, but it should be noted that the characterized clinical manifestations in EV71-infected neonatal monkeys directly contribute to clear experimental significance. Unlike studies in murine and cynomolgus monkey models in which other clinical symptoms such as paralysis and ataxia are common (Nagata et al., 2004; Wang et al., 2004), no definite neurological complications were noticed in the current study, except for a decrease in muscle tension of limbs that is difficult to quantify. Although EV71 strains used in those studies are adapted for murine and cynomolgus monkeys (Arita et al., 2005; Wang et al., 2004), there are differences exhibited in terms of molecular biological events when compared to the virus strain used in this rhesus monkey studies and that in human infection, and further investigation into the related mechanisms and the differences between the studies are required. However, one remarkable point that deserves to be mentioned is that the flaccid paralysis observed in murine and cynomolgus monkey studies is not a dominant manifestation in the population with HFMD reported recently (Kung et al., 2007), despite of some paralysis cases that had been reported in previous epidemics induced by B or C1 genotype virus in Europe (Kapusinszky et al., 2010; Ortner et al., 2009). In addition, the limited clinical manifestations showed that death and serious encephalomyelitis symptoms frequently displayed in human severe cases were failed to find in these neonatal monkeys, which leads us to raise the question of the variety of EV71 infection in rhesus monkey and human. However, all the data presented in current study are most likely to suggest a complete infectious process induced by EV71 in neonatal monkeys. These clinical symptoms and pathological findings, specifically in CNS presented in our work seem to allow for two presumptions: first, rhesus monkey might not be the natural host for EV71 infection and not as sensitive as human for virus infection; second, the 0.5% severe case reported in human by EV71 infection could not be simply defined in 8 neonatal monkeys in our experiment.

Our previous study in adult rhesus monkeys revealed a preference of EV71 infection to respiratory tract tissues (Supplemental Table 1) (Zhang et al., Submission) that is again confirmed in the current study of neonatal rhesus monkeys. The preference of EV71 infection to the respiratory tract in neonates was detected using viral loads and pathological changes in trachea tissues; other, higher viral loads were found in tissues of axillary lymph nodes, cervical lymph nodes, axillary and peritrachea brown adipose, upper arm muscle and pectoralis muscle. These higher viral loads were thought to be generated after initial infection by transmission of virus from the trachea to adjacent lymph nodes and other tissues (Fig. 2), which directly leads to viral transmission from involved peripheral nerves to the CNS. Therefore, the respiratory tract is presumed to be a potential natural infection route for EV71 in this model, which is further supported by lower viral loads detected in gastrointestinal tract and failure in noting remarkable pathological changes in other associated organs like the gaster and the small intestine. As evidenced in viral load analysis of the blood and EV71 antigen expressed in tissue samples from the trachea, spleen, lymph nodes and etc. (Supplemental Fig. 3), EV71 is presumed to enter into tissues of trachea and organs of associated respiratory tracts, thereafter to overall spread and transmit through the whole body. Viral load analysis revealed higher viral loads in brown adipose tissue (Fig. 2), which appears to suggest that brown adipose, a tissue primarily found in young humans and other primates, should also be the primary target tissue for viral replication. If this is the case, high infectious rates of EV71 in infants and young children (McMinn, 2002) seem explainable. Higher viral loads occur in tissues of blood vessels and skeletal muscles highlighting the capability of EV71 to infect many tissue types, which might correlate to a distribution of EV71 receptors in different tissues (Wong et al., 2010).

As shown in both pathological analysis in humans and studies in animal models, including rhesus monkeys in the presented work, the CNS has widely been identified as the main target organ for EV71 infection. Study in murine models proposed the potential mechanism of EV7 transmission from peripheral nerves to CNS via active retrograde axonal transport route (Chen et al., 2007). In our current work, higher viral loads were detected in brown adipose from day 4 p.i. followed by peaks occurred in blood vessels, upper arm and lower arm muscles and pectoralis muscles on day 7 p.i.. In parallel, viral loads in tissues of peripheral nerves like brachial plexus and intercostal nerves were increased dramatically (Fig. 3b), while viral load in the CNS exhibited a slight increase (Fig. 3a). On day 10 p.i. when viral loads in tissues of peripheral nerves, lymph nodes and brown adipose tissue declined (Fig. 2), the viral loads in a wide range of CNS samples, including every part of spinal cord, increased (Fig. 3) and displayed severe neuropathological lesions as indicated in histopathological examinations (Table 1). These findings allow for an argument that EV71 achieves its target of infecting the CNS in infected neonatal monkeys via a route of muscle tissue to peripheral nerves and finally reaching tissues in the CNS. Interestingly, regardless of papule or vesicle presence on the mouth, no virus was found in trigeminal nerves; regardless of the presence of very low viral titers in muscles of low limbs, no virus was detected in sciatic nerves. Taken these results together, it might be safe to conclude that EV71 would eventually infect a broad range of tissues in the CNS via peripheral nerves by active retrograde axonal transport route based upon its preference to respiratory tract infection and brown adipose tissues adjacent to upper limbs as primary target tissues.

To evaluate the reliability of using neonatal monkeys as the animal model, the feces taken from the EV71-infected monkeys, treated by sterilization and filtration, was used in infecting new neonatal monkeys via the respiratory tract, and clearly resulted in a complete infectious process consisting of the same steps and indicators in newly infected individuals. These results have enabled us to basically evaluate the reliability of this model in compliance with Koch's postulates and lead to the final confirmation. However, based upon the fact that some enteroviruses, especially poliovirus are capable of inducing neuropathological changes in CNS of rhesus monkeys upon infection that is similar to that indicated in our current work, it appears to be necessary to further specify rhesus monkey models for

EV71 infection. Although the recent data obtained in our laboratory showed negative results of Coxackievirus A16 infection in rhesus monkey (data not shown), the study of generic susceptibility might be required to further explore the neuropathological changes induced by other enterovirus A of human species in neonatal rhesus monkey.

In summary, our current study and previous work highlight the use of neonatal rhesus monkey as an animal model for EV71 infection that can be applied to provide objective indicators for observation and evaluation in interpreting the complete process of EV71 infection, shedding light on mechanisms of EV71 infection and development of new drugs and vaccines. Our work provides a valuable and significant basis for further study of the pathogenesis of EV71 in human patients with HFMD. Although the data describing EV71 transmission in humans and the associated mechanisms of pathogenesis are not fully elucidated, the fact that the systemic infectious process, infection of new hosts using fecal matter from infected hosts, and other collected indicators in a neonatal monkey model could repeatedly be duplicated to contribute to the reliability of this model.

Materials and methods

Viruses and cells

The EV71 virus used in this study was strain FY-23 that was isolated from a hematic secretion of the respiratory tract of an infected male child who presented with the clinical symptoms of severe cardiopulmonary collapse during an epidemic in Fuyang, China in May 2008 (Genbank accession number: EU812515.1) (Ma et al., 2009). The strain was purified using a 0.2-μm filter and identified as an EV71 C4 sub-genotype virus by RT-PCR before Vero cell inoculation. The virus grown in Vero cells was harvested for freezing at −20 °C when a typical cytopathic effect developed and the produced virus reached a concentration of $10^{6.5}$–$10^{7.5}$ cell culture infectious doses ($CCID_{50}$)/ml. The Vero cells were maintained in 0.5% MEM containing fetal bovine serum and grown to a confluent monolayer in a T-25 vessel or in 96-well plates for viral isolation and neutralizing antibody assays.

Virus titration and neutralization assay

EV71 harvested from cell culture or isolates from different organs and tissues of infected newborn rhesus monkeys were analyzed by performing a microtitration assay using a standard protocol (Arita et al., 2006). The neutralization test for the virus was performed according to the standard protocol (WHO, 1988); a mixture of diluted serum containing anti-EV71 antibodies and the virus at a titer of 500–1000 $CCID_{50}$ in 100 μl of phosphate-buffered saline (PBS) was incubated at 37 °C for 1 h. The cellular pathogenic effect (CPE) of the viruses was examined by inoculating the mixture onto Vero cells grown in 96-well plates. The plaque assay was performed in 6-well plates containing 90% confluent Vero monolayer cells. The cells were inoculated with samples from blood, throat swabs or feces. After 1 h incubation at 37 °C, the infection media were aspirated off and each well was then covered with 3 ml of agar overlay medium and incubated for 2 days at 37 °C in a CO_2 incubator. At the end of the incubation, the cells were fixed with formaldehyde and stained with 0.1% Crystal Violet as standard protocol (Hung et al., 2010).

Neonatal rhesus monkeys

The Office of Laboratory Animal Management of Yunnan Province, China approved the experimental animal procedure. A total of 14 healthy newborn rhesus monkeys with an average weight of 300 ± 350 g and an average age of 1–1.5 months were divided into two experimental groups, eight for the first group and four for the second group; two additional monkeys were used as negative controls. Each newborn monkey was kept in a single cage with its mother and fed according to the guidelines of the Committee of Experimental Animals at the Institute of Medical Biology, Chinese Academy of Medical Sciences (CAMS) (Gorska, 2000). All animals were kept in isolation for 2 weeks before the initiation of the study. A neutralization test was conducted to confirm that they did not have antibodies against EV71 prior to the experimental infections.

Infection in neonatal rhesus monkeys

The first experimental group of 8 monkeys was challenged with EV71 ($10^{4.5}$ $CCID_{50}$/monkey) via the respiratory tract by tracheoscopy according to standard protocol, in which the monkeys anesthetized with ketamine (10 mg/kg of body weight, Phoenix Pharmaceuticals, St. Joseph, Mo.) were infected by the 0.5 ml sterile saline consisting of viruses in a manner of instilling into the desired trachea via the biopsy channel of the bronchoscope. The 2 monkeys were used as uninfected negative controls. The infected neonates were breast-fed by female monkeys and monitored daily for clinical signs under un-anesthesia twice a day, such as body temperature measured by inserting a soft probe attached to Omron's electronic digital stick thermometers (MC-BOMR, Omron Co.) into rectal 2 cm from anal margin for 1 min each time, muscle tension of limbs, primary healthy status, papules or vesicles on limbs, etc. from day 2 post-infection (p.i.). The normal range of body temperature was defined based upon the reference (Li et al., 2005) and that of control animals. In parallel, venous blood samples were taken into EDTA coated capillary tubes daily for routine detection for biological indicators like blood count by Veterinary Multi-species Hematology System (Hemavet 950FS, Drew Scientific Co.), as well as viral loads. The normal percentage ranges of various blood cells were defined based upon the reference (Sibley et al., 1974). The pathogenic and histopathological examinations were performed on all the tissues and organs of neonates killed by electric shock on days 4, 7, 10, and 14 p.i. with anesthesia.

Histopathological examination and immunohistochemical analysis

Various tissue samples from the organs of the infected monkeys were fixed in 10% formalin in PBS, dehydrated in ethanol gradients and embedded in paraffin before obtaining 4-μm sections for further H–E staining. Histopathological analysis of the tissue sections from each organ was performed under a light microscope. Histological changes in the CNS (lesion score) were evaluated using a method recommended by the World Health Organization (WHO) (WHO, 1990), which included standard pathological evaluations of the cerebrum, cerebellum, brain stem and different sections of the spinal cord (Nagata et al., 2002). For the immunohistochemical analysis, the tissue samples were embedded in an optimal cutting temperature (OCT) compound (Miles Inc., Elkhart, Ind.) and frozen in liquid nitrogen. The frozen tissues were then cut into 4-μm sections, placed on poly-L-lysine-coated glass slides and fixed in 3.7% paraformaldehyde. The endogenous peroxidase activity of the tissues was inhibited by treatment with hydrogen peroxide (2.5%). The EV71 antigen was detected by mouse anti-enterovirus 71 monoclonal Antibody (Clone 10F0, Abcam, U.S.) and horseradish peroxidase (HRP)-conjugated anti-mouse IgG antibodies (Sigma, Deisenhofen, Germany) followed by color development with diaminobenzidine for the detection of the antigen–antibody reaction.

Extract of viral RNA and quantitative RT-PCR amplification

Viral RNA was extracted from 250 μl of fresh tissue homogenate (10%) and fecal homogenate (5%) from the experimental animals using the Qiagen RNeasy mini kit, according to the manufacturer's protocol (Qiagen, Hilden, Germany). The viral RNA was eluted in a final volume of 20 μl. For quantification, a single-tube, real-time Taqman RT-PCR assay was performed using the Taqman 1-step RT-PCR Master Mix in the 7500 Fast Real-time RT-PCR system (Applied

Biosystems, Foster City, CA). The reaction mixture contained the Taqman Universal PCR master mix, each primer at 200 nM, the FAM/TAMRA labeled probe at 100 nM (Takara Shuzo Co., Ltd., Shiga, Japan), and 2 μl of RNA in a 20-μl total reaction volume. The sequences for the EV71-specific primers are as follows: forward primer, 5′-ccctgaatgcggctaatcc-3′; probe, 5′-ccagcgggtagtgtgtcgtaacggg-3′; and reverse primer, 5′-attgtcaccataagcagcca-3′. The following protocol was used for all PCR assays: 5 min at 42 °C and 10 s at 95 °C, followed by 40 cycles at 95 °C for 5 s and 60 °C for 30 s. A standard reference curve was obtained by measurement of the serially diluted virus RNA generated by in vitro transcription from a DNA construct that contains the 5′-untranslated region (UTR). Based on the copy number of standard RNA, we then quantified the viral titer relative to the standard RNA by real-time RT-PCR analysis. Using this system, we measured each viral load separately in the infected tissue. All results were further confirmed in microtitration assay with tissue culture.

Infection of new individual monkeys by feces of EV71-infected neonatal monkeys

100 mg of feces of EV71-infected neonates at day 10 p.i. were acquired and suspended in 5 ml PBS for sterilization and filtration by a 0.2-μm filter. Each 500-μl solution was nasally inoculated into 4 negative neonates, confirmed by anti-EV71 antibody detection, and 2 to 2.5-month-old neonates. The infected neonates were monitored daily for the aforementioned clinical signs from day 2 until day 14 p.i. when two of the monkeys challenged via respiratory route were killed, and the other two were kept for daily virus detection in feces until day 30 p.i. In parallel, fecal samples from the breast-feeding monkeys for these 2 neonates were taken for daily virus detection from days 14 to 30 p.i.

Electron microscopy analysis

The tissue was prepared and fixed in a solution containing 0.5% glutaraldehyde, 4% paraformaldehyde, and 0.1 M of sodium phosphate buffer (pH 7.6) on ice for 1 h. After washes with 4% sucrose in 0.1 M of phosphate buffer, the tissue was decalcified with 2.5% EDTA solution for 5 days. After three washes, the samples were fixed with 2% osmium tetraoxide on ice for 1 h and dehydrated with a series of ethanol gradients. For transmission electron microscopy, the tissues were embedded in Epon 812 resin mixture, and ultrathin (70-nm) sections were cut with Leica EM UC6 ultramicrotome (Leica Co., Austria). The ultrathin sections were stained with 2% uranyl acetate in 70% ethanol for 5 min at room temperature and then in Reynold's lead for 5 min at room temperature. Sections were analyzed with H-7650 transmission electron microscope (HITACHI, Japan).

Supplementary materials related to this article can be found online at doi:10.1016/j.virol.2010.12.058.

Acknowledgments

This work was supported by National S&T Major Project (2008ZX10004-014) and National Basic Research Program (2011CB504903).

References

Arita, M., Shimizu, H., Nagata, N., Ami, Y., Suzaki, Y., Sata, T., Iwasaki, T., Miyamura, T., 2005. Temperature-sensitive mutants of enterovirus 71 show attenuation in cynomolgus monkeys. J. Gen. Virol. 86 (Pt 5), 1391–1401.

Arita, M., Nagata, N., Sata, T., Miyamura, T., Shimizu, H., 2006. Quantitative analysis of poliomyelitis-like paralysis in mice induced by a poliovirus replicon. J. Gen. Virol. 87 (Pt 11), 3317–3327.

Arita, M., Nagata, N., Iwata, N., Ami, Y., Suzaki, Y., Mizuta, K., Iwasaki, T., Sata, T., Wakita, T., Shimizu, H., 2007. An attenuated strain of enterovirus 71 belonging to genotype a showed a broad spectrum of antigenicity with attenuated neurovirulence in cynomolgus monkeys. J. Virol. 81 (17), 9386–9395.

Asher, L.V., Binn, L.N., Mensing, T.L., Marchwicki, R.H., Vassell, R.A., Young, G.D., 1995. Pathogenesis of hepatitis A in orally inoculated owl monkeys (*Aotus trivirgatus*). J. Med. Virol. 47 (3), 260–268.

Bodian, D., 1955. Emerging concept of poliomyelitis infection. Science 122 (3159), 105–108.

CDC, 1998. Deaths among children during an outbreak of hand, foot, and mouth disease — Taiwan, Republic of China, April–July 1998. MMWR Morb. Mortal. Wkly Rep. 47, 629–632.

Chan, L.G., Parashar, U.D., Lye, M.S., Ong, F.G., Zaki, S.R., Alexander, J.P., Ho, K.K., Han, L.L., Pallansch, M.A., Suleiman, A.B., Jegathesan, M., Anderson, L.J., 2000. Deaths of children during an outbreak of hand, foot, and mouth disease in Sarawak, Malaysia: clinical and pathological characteristics of the disease. For the Outbreak Study Group. Clin. Infect. Dis. 31 (3), 678–683.

Chen, Y.C., Yu, C.K., Wang, Y.F., Liu, C.C., Su, I.J., Lei, H.Y., 2004. A murine oral enterovirus 71 infection model with central nervous system involvement. J. Gen. Virol. 85 (Pt 1), 69–77.

Chen, C.S., Yao, Y.C., Lin, S.C., Lee, Y.P., Wang, Y.F., Wang, J.R., Liu, C.C., Lei, H.Y., Yu, C.K., 2007. Retrograde axonal transport: a major transmission route of enterovirus 71 in mice. J. Virol. 81 (17), 8996–9003.

Compton, T., Kurt-Jones, E.A., Boehme, K.W., Belko, J., Latz, E., Golenbock, D.T., Finberg, R.W., 2003. Human cytomegalovirus activates inflammatory cytokine responses via CD14 and Toll-like receptor 2. J. Virol. 77 (8), 4588–4596.

Couderc, T., Christodoulou, C., Kopecka, H., Marsden, S., Taffs, L.F., Crainic, R., Horaud, F., 1989. Molecular pathogenesis of neural lesions induced by poliovirus type 1. J. Gen. Virol. 70 (Pt 11), 2907–2918.

Ding, N.Z., Wang, X.M., Sun, S.W., Song, Q., Li, S.N., He, C.Q., 2009. Appearance of mosaic enterovirus 71 in the 2008 outbreak of China. Virus Res. 145 (1), 157–161.

Dragunsky, E., Taffs, R., Chernokhvostova, Y., Nomura, T., Hioki, K., Gardner, D., Norwood, L., Levenbook, I., 1996. A poliovirus-susceptible transgenic mouse model as a possible replacement for the monkey neurovirulence test of oral poliovirus vaccine. Biologicals 24 (2), 77–86.

Gorska, P., 2000. Principles in laboratory animal research for experimental purposes. Med. Sci. Monit. 6 (1), 171–180.

Han, J., Ma, X.J., Wan, J.F., Liu, Y.H., Han, Y.L., Chen, C., Tian, C., Gao, C., Wang, M., Dong, X.P., 2010. Long persistence of EV71 specific nucleotides in respiratory and feces samples of the patients with Hand–Foot–Mouth Disease after recovery. BMC Infect. Dis. 10, 178.

Hashimoto, I., Hagiwara, A., 1983. Comparative studies on the neurovirulence of temperature-sensitive and temperature-resistant viruses of enterovirus 71 in monkeys. Acta Neuropathol. 60 (3–4), 266–270.

Ho, M., Chen, E.R., Hsu, K.H., Twu, S.J., Chen, K.T., Tsai, S.F., Wang, J.R., Shih, S.R., 1999. An epidemic of enterovirus 71 infection in Taiwan. Taiwan Enterovirus Epidemic Working Group. N. Engl. J. Med. 341 (13), 929–935.

Horie, H., Koike, S., Kurata, T., Sato-Yoshida, Y., Ise, I., Ota, Y., Abe, S., Hioki, K., Kato, H., Taya, C., et al., 1994. Transgenic mice carrying the human poliovirus receptor: new animal models for study of poliovirus neurovirulence. J. Virol. 68 (2), 681–688.

Hsueh, C., Jung, S.M., Shih, S.R., Kuo, T.T., Shieh, W.J., Zaki, S., Lin, T.Y., Chang, L.Y., Ning, H.C., Yen, D.C., 2000. Acute encephalomyelitis during an outbreak of enterovirus type 71 infection in Taiwan: report of an autopsy case with pathologic, immunofluorescence, and molecular studies. Mod. Pathol. 13 (11), 1200–1205.

Hung, H.C., Chen, T.C., Fang, M.Y., Yen, K.J., Shih, S.R., Hsu, J.T., Tseng, C.P., 2010. Inhibition of enterovirus 71 replication and the viral 3D polymerase by aurintricarboxylic acid. J. Antimicrob. Chemother. 65 (4), 676–683.

Kapusinszky, B., Szomor, K.N., Farkas, A., Takacs, M., Berencsi, G., 2010. Detection of non-polio enteroviruses in Hungary 2000–2008 and molecular epidemiology of enterovirus 71, coxsackievirus A16, and echovirus 30. Virus Genes 40 (2), 163–173.

Kung, C.M., King, C.C., Lee, C.N., Huang, L.M., Lee, P.I., Kao, C.L., 2007. Differences in replication capacity between enterovirus 71 isolates obtained from patients with encephalitis and those obtained from patients with herpangina in Taiwan. J. Med. Virol. 79 (1), 60–68.

Li, C.C., Yang, M.Y., Chen, R.F., Lin, T.Y., Tsao, K.C., Ning, H.C., Liu, H.C., Lin, S.F., Yeh, W.T., Chu, Y.T., Yang, K.D., 2002. Clinical manifestations and laboratory assessment in an enterovirus 71 outbreak in southern Taiwan. Scand. J. Infect. Dis. 34 (2), 104–109.

Li, B.J., Tang, Q., Cheng, D., Qin, C., Xie, F.Y., Wei, Q., Xu, J., Liu, Y., Zheng, B.J., Woodle, M.C., Zhong, N., Lu, P.Y., 2005. Using siRNA in prophylactic and therapeutic regimens against SARS coronavirus in Rhesus macaque. Nat. Med. 11 (9), 944–951.

Lin, T.Y., Hsia, S.H., Huang, Y.C., Wu, C.T., Chang, L.Y., 2003a. Proinflammatory cytokine reactions in enterovirus 71 infections of the central nervous system. Clin. Infect. Dis. 36 (3), 269–274.

Lin, T.Y., Twu, S.J., Ho, M.S., Chang, L.Y., Lee, C.Y., 2003b. Enterovirus 71 outbreaks, Taiwan: occurrence and recognition. Emerg. Infect. Dis. 9 (3), 291–293.

Lin, M.T., Wang, J.K., Lu, F.L., Wu, E.T., Yeh, S.J., Lee, W.L., Wu, J.M., Wu, M.H., 2006. Heart rate variability monitoring in the detection of central nervous system complications in children with enterovirus infection. J. Crit. Care 21 (3), 280–286.

Liu, C.C., Tseng, H.W., Wang, S.M., Wang, J.R., Su, I.J., 2000. An outbreak of enterovirus 71 infection in Taiwan, 1998: epidemiologic and clinical manifestations. J. Clin. Virol. 17 (1), 23–30.

Ma, S.-h., Liu, J.-s., Wang, J.-j., Shi, H.-j., Yang, H.-j., Chen, J.-y., Liu, L.-d., Li, Q.-h., 2009. Genetic analysis of the VP1 region of human enterovirus 71 strains isolated in Fuyang, China, during 2008. Virol. Sin. 24 (3), 162–170.

McMinn, P.C., 2002. An overview of the evolution of enterovirus 71 and its clinical and public health significance. FEMS Microbiol. Rev. 26 (1), 91–107.

Mena, I., Fischer, C., Gebhard, J.R., Perry, C.M., Harkins, S., Whitton, J.L., 2000. Coxsackievirus infection of the pancreas: evaluation of receptor expression, pathogenesis, and immunopathology. Virology 271 (2), 276–288.

Nagata, N., Shimizu, H., Ami, Y., Tano, Y., Harashima, A., Suzaki, Y., Sato, Y., Miyamura, T., Sata, T., Iwasaki, T., 2002. Pyramidal and extrapyramidal involvement in experimental infection of cynomolgus monkeys with enterovirus 71. J. Med. Virol. 67 (2), 207–216.

Nagata, N., Iwasaki, T., Ami, Y., Tano, Y., Harashima, A., Suzaki, Y., Sato, Y., Hasegawa, H., Sata, T., Miyamura, T., Shimizu, H., 2004. Differential localization of neurons susceptible to enterovirus 71 and poliovirus type 1 in the central nervous system of cynomolgus monkeys after intravenous inoculation. J. Gen. Virol. 85 (Pt 10), 2981–2989.

Ong, K.C., Badmanathan, M., Devi, S., Leong, K.L., Cardosa, M.J., Wong, K.T., 2008. Pathologic characterization of a murine model of human enterovirus 71 encephalomyelitis. J. Neuropathol. Exp. Neurol. 67 (6), 532–542.

Ooi, M.H., Solomon, T., Podin, Y., Mohan, A., Akin, W., Yusuf, M.A., del Sel, S., Kontol, K.M., Lai, B.F., Clear, D., Chieng, C.H., Blake, E., Perera, D., Wong, S.C., Cardosa, J., 2007. Evaluation of different clinical sample types in diagnosis of human enterovirus 71-associated hand–foot-and-mouth disease. J. Clin. Microbiol. 45 (6), 1858–1866.

Ortner, B., Huang, C.W., Schmid, D., Mutz, I., Wewalka, G., Allerberger, F., Yang, J.Y., Huemer, H.P., 2009. Epidemiology of enterovirus types causing neurological disease in Austria 1999–2007: detection of clusters of echovirus 30 and enterovirus 71 and analysis of prevalent genotypes. J. Med. Virol. 81 (2), 317–324.

Ouzilou, L., Caliot, E., Pelletier, I., Prevost, M.C., Pringault, E., Colbere-Garapin, F., 2002. Poliovirus transcytosis through M-like cells. J. Gen. Virol. 83 (Pt 9), 2177–2182.

Racaniello, V.R., 2006. One hundred years of poliovirus pathogenesis. Virology 344 (1), 9–16.

Shimizu, H., Utama, A., Yoshii, K., Yoshida, H., Yoneyama, T., Sinniah, M., Yusof, M.A., Okuno, Y., Okabe, N., Shih, S.R., Chen, H.Y., Wang, G.R., Kao, C.L., Chang, K.S., Miyamura, T., Hagiwara, A., 1999. Enterovirus 71 from fatal and nonfatal cases of hand, foot and mouth disease epidemics in Malaysia, Japan and Taiwan in 1997–1998. Jpn J. Infect. Dis. 52 (1), 12–15.

Shwartzman, G., Aronson, S.M., Teodoru, C.V., Adler, M., Jahiel, R., 1955. Endocrinological aspects of pathogenesis of experimental poliomyelitis. Ann. NY Acad. Sci. 61 (4), 869–876.

Sibley, P.L., Traina, V.M., Parekh, C.K., 1974. Normal range and variability of hematologic and blood-chemical parameters from beagle dogs and rhesus monkeys. Toxicol. Pathol. 2, 22–28.

Wang, Y.F., Chou, C.T., Lei, H.Y., Liu, C.C., Wang, S.M., Yan, J.J., Su, I.J., Wang, J.R., Yeh, T.M., Chen, S.H., Yu, C.K., 2004. A mouse-adapted enterovirus 71 strain causes neurological disease in mice after oral infection. J. Virol. 78 (15), 7916–7924.

Whitton, J.L., Cornell, C.T., Feuer, R., 2005. Host and virus determinants of picornavirus pathogenesis and tropism. Nat. Rev. Microbiol. 3 (10), 765–776.

WHO, 1988. Procedure for Using the Lyophilized LBM Pools for Typing Enterovirus, Geneva.

WHO, 1990. Requirements for poliomyelitis vaccine (oral). WHO Tech. Rep. Ser. 800, 30–65.

Wong, K.T., Munisamy, B., Ong, K.C., Kojima, H., Noriyo, N., Chua, K.B., Ong, B.B., Nagashima, K., 2008. The distribution of inflammation and virus in human enterovirus 71 encephalomyelitis suggests possible viral spread by neural pathways. J. Neuropathol. Exp. Neurol. 67 (2), 162–169.

Wong, S.S., Yip, C.C., Lau, S.K., Yuen, K.Y., 2010. Human enterovirus 71 and hand, foot and mouth disease. Epidemiol. Infect. 138 (8), 1071–1089.

Xu, J., Qian, Y., Wang, S., Serrano, J.M., Li, W., Huang, Z., Lu, S., 2010. EV71: an emerging infectious disease vaccine target in the Far East? Vaccine 28 (20), 3516–3521.

Yang, F., Ren, L., Xiong, Z., Li, J., Xiao, Y., Zhao, R., He, Y., Bu, G., Zhou, S., Wang, J., Qi, J., 2009. Enterovirus 71 outbreak in the People's Republic of China in 2008. J. Clin. Microbiol. 47 (7), 2351–2352.

Zhang, Y., Cui, W., Liu, L., Wang, J., Zhao, H., Liao, Y., Na, R., Dong, C., Wang, L., Xie, Z., Gao, J., Cui, P., Zhang, X., and Li, Q. (Submission). Pathogenesis study of enterovirus 71 infection in rhesus monkeys. *Submission*.